

CORRESPONDENCE OPEN



ATM germline variants in a young adult with chronic lymphocytic leukemia: 8 years of genomic evolution

© The Author(s) 2022

Blood Cancer Journal (2022) 12:90; <https://doi.org/10.1038/s41408-022-00686-6>

Chronic lymphocytic leukemia (CLL) is a disease commonly diagnosed in the elderly with a median age of ~70 years. However, CLL can also be detected in adolescent and young adults (AYA). According to different studies, 0.85–3.7% of patients with CLL are diagnosed in AYA and 3% of these patients had a first-degree relative with CLL [1]. Families with multiple individuals affected with CLL and other related B-cell tumors have been described with contradictory findings regarding their potential early age at diagnosis [2]. Despite these observations, our knowledge about the molecular profile and predisposing factors in AYA CLL is scarce [3, 4].

Comprehensive studies have dissected the (epi)genomic, and transcriptomic landscape of CLL [5]. Approximately 9–18% of CLL harbor del(11q) which occurs in younger patients with bulky disease and poor survival. These deletions are frequently associated with germline and acquired mutations of *ATM* [6]. Patients with the inherited disorder ataxia telangiectasia have biallelic alterations of the *ATM* gene and increased susceptibility to lymphoid malignancies [7]. Rare, protein-coding germline *ATM* variants are associated with CLL in adults [8]. However, *ATM* mutations are uncommon in familial CLL [9].

Here, we describe an 18-year-old woman diagnosed with CLL whose family history included a younger brother with B-cell acute lymphoblastic leukemia (B-ALL) and other family members carrying germline *ATM* mutations. A combination of whole-genome and single-cell characterization of this CLL at diagnosis and during the course of the disease provided an opportunity to understand the genomic profile of AYA CLL and the sequence of events driving its evolution.

An 18-year-old female was diagnosed with CLL, Binet-Rai stage AI, at another institution, in the study of a lymphocytosis detected in a routine blood test. She had a past medical history of anxiety-depressive syndrome during childhood and chronic headache, but no neurological symptoms were reported. The patient had a younger brother diagnosed with B-ALL when he was 3 years old, and was in complete remission 13 years later, and an older sister with epilepsy. Her parents were both healthy.

At the time of CLL diagnosis, the patient was asymptomatic with a normal physical exam. Her white blood cell count (WBC) was $9.08 \times 10^9/L$, with 75% lymphocytes. Hemoglobin and platelet count were normal. Peripheral blood smear showed small atypical lymphocytes consistent with CLL, which phenotype was CD5⁺, CD23⁺, CD43⁺, CD200⁺, CD10⁻, CD20 and CD22 weakly positive with weak kappa light chain restriction. The fluorescence in situ hybridization (FISH) analysis for *ATM* (11q22), *D12Z3* (cen 12), *DLEU* (13q14.3), *LAMP1* (13q34), and *TP53* (17p13) were normal. One year after diagnosis, the patient received two cycles of rituximab

plus fludarabine and cyclophosphamide (FCR) due to progressive disease, achieving a complete remission. The patient was then referred to our hospital. Physical examination was normal without evidence of lymphadenopathy or splenomegaly. WBC count was $2 \times 10^9/L$ with 10% lymphocytes, hemoglobin 117 g/L, and normal platelet count. Watchful waiting was recommended. She was diagnosed of a CLL as a result of the study of a lymphocytosis in a routine analysis requested by her gynecologist. Fue diagnosticada de CLL como resultado del estudio de una linfocitosis en un análisis de rutina solicitado por su ginecólogo. She was diagnosed with CLL in the wake of the study of a lymphocytosis in a routine analysis requested by her gynecologist. Five years later, the CLL progressed with increased lymphocytosis, inguinal, axillary, and laterocervical lymphadenopathy (2–3 cm) and splenomegaly of 4 cm below the costal margin. At that time, the karyotype was 46, XX, del(13)(q12q21)[6]/46, XX[10] and a heterozygous del(13q14.3) was detected by FISH in 92% of nuclei. FISH for *ATM*, *D12Z3*, and *TP53* were normal and no *TP53* mutations were observed. The sequence of the IGHV3-21 with 100% homology to the germline, not belonging to any major stereotype subset (Supplementary Tables 1, 2). Due to CLL progression, ibrutinib 420 mg per day was started and the patient achieved a partial response. However, after 20 months, ibrutinib had to be discontinued due to the severe diarrhea and acalabrutinib 100 mg every 12 h was started. Progression of CLL was observed after 13 months of treatment and rituximab and venetoclax were initiated (Fig. 1A).

The patient was included in the CLL program of the International Cancer Genome Consortium and the whole genomes of the germline and tumor sample at diagnosis were sequenced [5]. No somatically-acquired driver alterations were detected but three germline *ATM* mutations were identified, including a pathogenic 28-base frameshift deletion (p.N3003Dfs*6) and two missense single nucleotide variants (p.K2204M and p.Y1961C). Although the p.K2204M missense variant has not been identified in previous studies, the p.Y1961C has been reported in a CLL patient and its modeling showed reduced ATM kinase activity [10]. Based on this result, we studied the segregation of these mutations in the family members by Sanger sequencing. The mother harbored the frameshift deletion, while the father and the sister carried the two missense variants. Both the patient and her brother with B-ALL inherited all three variants (Fig. 1B, Supplementary Tables 3, 4). A milder ataxia telangiectasia phenotype, where the disease progresses at a slower pace, has been observed in patients with reduced levels of ATM kinase activity [11]. At time of last follow-up the two siblings (28 and 16 years old) had not developed neurological symptoms.

To better unfold the contribution of somatic alterations during the evolution of the disease, whole-genome sequencing (WGS) was performed at 3 additional time points over a period of 8 years and complemented with single-cell DNA-sequencing (Fig. 1A, Supplementary Table 1). Using a longitudinal sample-aware

Received: 11 May 2022 Revised: 13 May 2022 Accepted: 25 May 2022
Published online: 07 June 2022

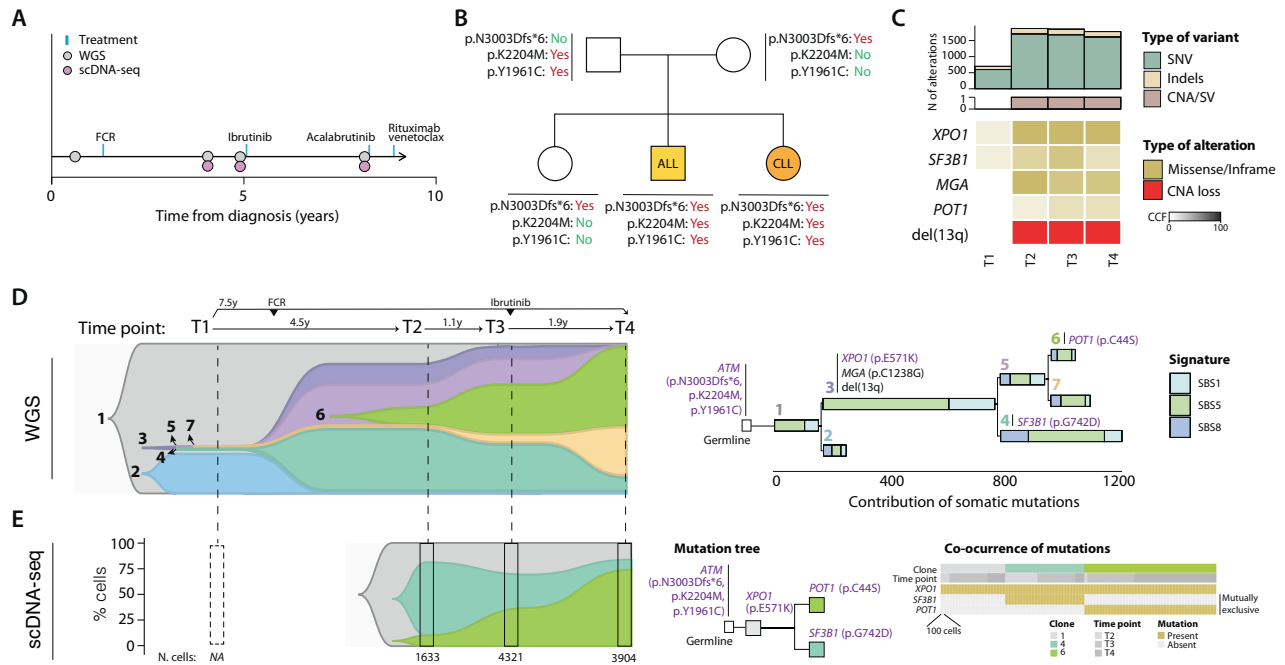


Fig. 1 Clinical course and genomic characterization. **A** Clinical course and samples analyzed. **B** Pedigree tree of germline variants in *ATM*. The two missense variants carried by the mother and the frameshift variant from the father were inherited by the chronic lymphocytic leukemia (CLL) case studied and her brother that developed acute lymphoblastic leukemia (ALL). **C** The upper barplots show the number of mutations [single nucleotide variants (SNV) and short insertions and deletions (indels)] and copy number alterations (CNA) or structural variants (SV) at each time point. The lower oncoprint shows the driver alterations, the transparency of the color is proportional to the cancer cell fraction (CCF). **D** The fishplot [left] depicts the subclonal architecture and clonal dynamics inferred from WGS. Each vertical line represents a time point analyzed. Each subclone is painted in a different color, and its height is proportional to the CCF at each time point. The upper-right tree shows the phylogeny of the tumor cell subpopulations, the length of the branches is proportional to the number of acquired SNV, and they are colored by contribution of mutational signatures identified in CLL [right]. The clock-like signatures SBS1 and SBS5 contributed most of the mutations acquired. **E** The fishplot (left) shows the clonal dynamics measured by single-cell analysis. For each available time point, the integrated barplot shows the proportion of cells harboring each specific combination of alterations in the driver genes illustrated on the “Mutation tree” (middle). The total number of analyzed cells at each analyzed sample is shown at the bottom. The “Co-occurrence of mutations” plot (right) indicates the presence or absence of mutations in each cell. For illustrative purposes, cells have been merged in bins of 100.

mutation calling pipeline that increases sensitivity, we identified 689 genome-wide and 7 non-synonymous variants in the WGS at diagnosis, increasing up to 1779 genome-wide and 18 non-synonymous at the latest sample analyzed. Among them, four mutations were found in CLL driver genes over the course of the disease: *XPO1* (p.E571K), *SF3B1* (p.G742D), *MGA* (p.C1238G), and *POT1* (p.C44S). The mutations in *XPO1* and *SF3B1* were already present at diagnosis but were missed in our previous study [5] due to their very low frequencies. After 4 years (time point 2), their clonal size expanded, and the remaining two driver mutations in *MGA* and *POT1* were detected. Regarding structural alterations, only del(13q) was clonally detected at the second time point and onwards (Fig. 1C, Supplementary Methods, Supplementary Tables 5, 8).

Somatic driver alterations were present at different allele frequencies through the disease course, suggesting an ongoing clonal evolution driving the pre- and post-treatment progression of the disease. To dissect the underlying clonal evolution, we reconstructed the subclonal evolution and explored the mutational processes active during the CLL course (Fig. 1D, Supplementary Methods, Supplementary Tables 9, 10). This analysis revealed a branching pattern of evolution in which the founding CLL clone did not carry any recognized driver alteration beyond the *ATM* germline variants. Additionally, two minor subclones were already present at diagnosis: subclone #3 carrying del(13q), *XPO1* and *MGA*, and subclone #4 which originated from subclone #3 and acquired the *SF3B1* mutation (Fig. 1D). These lineage trajectories are in line with previous literature in which *ATM* loss preceded del(13q) in a familial CLL study [12] and with a recently

described combinatorial effect of *ATM* loss and *SF3B1* mutation [13]. Intriguingly, these small subclones at diagnosis expanded after treatment with FCR, that, on the other hand, reduced or eliminated the initial subclones #1 and #2, with no additional CLL drivers, suggesting that decreased competition allowed the expansion of subclones carrying potent drivers. Of note, subclone #4 carrying the *SF3B1* mutation represented the largest subpopulation of cells at relapse post-treatment with FCR (time point 2), in line with the poor prognosis of *SF3B1* mutated cases under FCR therapy [14]. Nonetheless, this subclone slightly diminished at time point 3 and was virtually eradicated at time point 4 after treatment with ibrutinib, which is in line with the higher sensitivity of *SF3B1* mutated CLL cells to BCR inhibition in vitro [13]. Additional diversification was observed in subclone #3 at time point 2 which led to the emergence of subclone #6 harboring the *POT1* mutation. This subclone expanded under ibrutinib treatment and accounted for 54% at the last time point analyzed 3 years after its detection (Fig. 1D). To confirm these evolutionary trajectories, we performed single-cell DNA-sequencing of 32 CLL driver genes and identified the reported mutations in *XPO1*, *SF3B1*, and *POT1* [note that *MGA* was not included in the commercial gene panel used]. This single-cell analysis confirmed the timing of acquisition of these driver mutations and the clonal dynamics inferred from WGS (Fig. 1E, Supplementary Methods, Supplementary Tables 11, 14).

Here we have reported the 8-year genomic evolution of a CLL diagnosed in a young patient that inherited three *ATM* variants, two of them previously reported to inactivate or reduce *ATM*

activity (Supplementary Table 4) [10]. The combination of these three germline *ATM* variants predisposed to two distinct B-cell neoplasm in two siblings. These *ATM* variants represented the only recognized driver events in the founding CLL clone, suggesting that *ATM* inactivation might be a genomic factor contributing to CLL initiation. Tumor evolution and disease progression was dictated by the acquisition of secondary driver alterations, which could be detected in small subclones years before their expansion, and by different types of treatment that influenced subsequent clonal dynamics. Of note, this patient responded well to initial FCR therapy and later to ibrutinib treatment when *ATM* inactivation was accompanied by an *SF3B1* mutation, which is in line with the favorable clinical behavior of del(11q) CLL under BTK inhibitors [15]. Altogether, the lack of somatically-acquired, genetic driver alterations in the founding CLL of this patient emphasizes the need to study the germline as well as non-genetic aspects of the tumors to further understand the mechanisms leading to CLL.

ACCESSION NUMBER

The WGS and single-cell DNA-sequencing data have been deposited to the European Genome-phenome Archive (EGA) under the accession code EGAS00001006268.

Romina Royo^{1,10}, Laura Magnano^{2,3,4,10}, Julio Delgado^{2,3,4,5}, Sara Ruiz-Gil⁶, Josep Ll. Gelpi^{1,5}, Holger Heyn^{6,7}, Malcom A. Taylor⁸, Tatjana Stankovic⁸, Xose S. Puente^{3,9}, Ferran Nadeu^{2,3,11} and Elías Campo^{2,3,4,5,11} ✉
¹Barcelona Supercomputing Center (BSC), Barcelona, Spain. ²Institut d'Investigacions Biomèdiques August Pi i Sunyer (IDIBAPS), Barcelona, Spain. ³Centro de Investigación Biomédica en Red de Cáncer (CIBERONC), Madrid, Spain. ⁴Hospital Clínic of Barcelona, Barcelona, Spain. ⁵Universitat de Barcelona, Barcelona, Spain. ⁶CNAG-CRG, Centre for Genomic Regulation (CRG), Barcelona Institute of Science and Technology (BIST), Barcelona, Spain. ⁷Universitat Pompeu Fabra (UPF), Barcelona, Spain. ⁸Institute of Cancer and Genomic Sciences, University of Birmingham, Edgbaston, UK. ⁹Departamento de Bioquímica y Biología Molecular, Instituto Universitario de Oncología, Universidad de Oviedo, Oviedo, Spain. ¹⁰These authors contributed equally: Romina Royo, Laura Magnano. ¹¹These authors jointly supervised this work: Ferran Nadeu, Elías Campo. ✉email: ecampo@clinic.cat

REFERENCES

- Cherng HJ, Jammal N, Paul S, Wang X, Sasaki K, Thompson P, et al. Clinical and molecular characteristics and treatment patterns of adolescent and young adult patients with chronic lymphocytic leukaemia. *Br J Haematol.* 2021;194:61–68.
- Goldin LR, Bjorkholm M, Kristinsson SY, Turesson I, Landgren O. Elevated risk of chronic lymphocytic leukemia and other indolent non-Hodgkin's lymphomas among relatives of patients with chronic lymphocytic leukemia. *Haematologica.* 2009;94:647–53.
- Luskin M, Wertheim G, Morrisette J, Daber R, Biegel J, Wilmoth D, et al. CLL/SLL diagnosed in an adolescent. *Pediatr Blood Cancer.* 2014;61:1107–10.
- Nassereddine S, Dunleavy K. A case of chronic lymphocytic leukemia in an AYA patient. *Clin Lymphoma Myeloma Leuk.* 2019;19:S280.
- Puente XS, Beà S, Valdés-Mas R, Villamor N, Gutiérrez-Abril J, Martín-Subero JI, et al. Non-coding recurrent mutations in chronic lymphocytic leukaemia. *Nature.* 2015;526:519–24.
- Skowronska A, Austen B, Powell JE, Weston V, Oscier DG, Dyer MJS, et al. *ATM* germline heterozygosity does not play a role in chronic lymphocytic leukemia initiation but influences rapid disease progression through loss of the remaining *ATM* allele. *Haematologica.* 2012;97:142–6.
- Reiman A, Srinivasan V, Barone G, Last JI, Wootton LL, Davies EG, et al. Lymphoid tumours and breast cancer in ataxia telangiectasia; substantial protective effect of residual *ATM* kinase activity against childhood tumours. *Br J Cancer.* 2011;105:586–91.
- Tiao G, Improgo MR, Kasar S, Poh W, Kamburov A, Landau DA, et al. Rare germline variants in *ATM* are associated with chronic lymphocytic leukemia. *Leukemia.* 2017;31:2244–7.
- Yuille MR, Condie A, Hudson CD, Bradshaw PS, Stone EM, Matutes E, et al. *ATM* mutations are rare in familial chronic lymphocytic leukemia. *Blood.* 2002;100:603–9.
- Barone G, Groom A, Reiman A, Srinivasan V, Byrd PJ, Taylor AMR. Modeling *ATM* mutant proteins from missense changes confirms retained kinase activity. *Hum Mutat.* 2009;30:1222–30.
- Stewart GS, Last JIK, Stankovic T, Haites N, Kidd AMJ, Byrd PJ, et al. Residual ataxia telangiectasia mutated protein function in cells from ataxia telangiectasia patients, with 5762ins137 and 7271T→G mutations, showing a less severe phenotype. *J Biol Chem.* 2001;276:30133–41.
- Kostopoulos IV, Tsakiridou AA, Pavlidis D, Megalaki A, Papadhimitriou SI. Familial chronic lymphocytic leukemia in two siblings with *ATM/13q14* deletion and a similar pattern of clonal evolution. *Blood Cancer J.* 2015;5:e322–e322.
- Yin S, Gamba RG, Sun J, Martinez AZ, Cartun ZJ, Regis FFD, et al. A murine model of chronic lymphocytic leukemia based on B cell-restricted expression of *Sf3b1* mutation and *Atm* deletion. *Cancer Cell.* 2019;35:283–296.e5.
- Stilgenbauer S, Schnaiter A, Paschka P, Zenz T, Rossi M, Döhner K, et al. Gene mutations and treatment outcome in chronic lymphocytic leukemia: results from the CLL8 trial. *Blood.* 2014;123:3247–54.
- Kipps TJ, Hillmen P, Demirkan F, Grosicki S, Coutre SE, Barrientos JC, et al. 11q deletion (del11q) is not a prognostic factor for adverse outcomes for patients with chronic lymphocytic leukemia/small lymphocytic lymphoma (CLL/SLL) treated with ibrutinib: pooled data from 3 randomized phase 3 studies. *Blood.* 2016;128:2042–2042.

ACKNOWLEDGEMENTS

The authors thank the Hematopathology Collection registered at the Biobank of Hospital Clínic—Institut d'Investigacions Biomèdiques August Pi i Sunyer (IDIBAPS) as well as Sílvia Martín for the technical support. This study was supported by the “la Caixa” Foundation (CLLEvolution-LCF/PR/HR17/52150017, Health Research 2017 Program HR17-00221, to EC), the European Research Council (ERC) under the European Union's Horizon 2020 research and innovation program (810287, BCLLatlas, to EC, and HH), CERCA Program/Generalitat de Catalunya, Generalitat de Catalunya Suport Grups de Recerca AGAUR 2017-SGR-1142 (to EC), CIBERONC (CB16/12/00225 to EC), Ministerio de Ciencia e Innovación PID2020-117185RB-I00 (to XSP), FEDER: European Regional Development Fund “Una manera de hacer Europa”, and Fundación Asociación Española Contra el Cáncer FUNCAR-PRYGN211258SUAR (to XSP). The authors thankfully acknowledge the computer resources at MareNostrum4 and the technical support provided by Barcelona Supercomputing Center (RES activity BCV-2018-3-0001). FN acknowledge research support from the American Association for Cancer Research (2021 AACR-Amgen Fellowship in Clinical/Translational Cancer Research, Grant Number 21-40-11-NADE), the European Hematology Association (EHA Junior Research Grant 2021, Grant Number RG-202012-00245), and the Lady Tata Memorial Trust (International Award for Research in Leukemia 2021–2022, Grant Number LADY_TATA_21_3223). EC is an Academia Researcher of the “Institució Catalana de Recerca i Estudis Avançats” (ICREA) of the Generalitat de Catalunya. This work was partially developed at the Centre Esther Koplowitz (CEK, Barcelona, Spain).

AUTHOR CONTRIBUTIONS

RR collected data, analyzed data, and wrote the manuscript. LM and JD collected samples and clinical data, and wrote the manuscript. SR-G and HH performed single-cell experiments. MAT and TS interpreted data. JLLG and XSP analyzed and interpreted data. FN and EC designed the study, collected and analyzed data, wrote the manuscript, and supervised the research. All authors reviewed and approved the manuscript.

COMPETING INTERESTS

HH is co-founder of Omniscope and consultant to MirXES. XSP is co-founder of and holds an equity stake in DREAMgenics. FN has received honoraria from Janssen for speaking at educational activities. EC has been a consultant for Takeda, NanoString, AbbVie, and Illumina; has received honoraria from Janssen, EUSPharma, and Roche for speaking at educational activities; and is an inventor on a Lymphoma and Leukemia Molecular Profiling Project patent “Method for subtyping lymphoma subtypes by means of expression profiling” (PCT/US2014/64161) not related to this project. The remaining authors declare no competing interests.

ADDITIONAL INFORMATION

Supplementary information The online version contains supplementary material available at <https://doi.org/10.1038/s41408-022-00686-6>.

Correspondence and requests for materials should be addressed to Elías Campo.

Reprints and permission information is available at <http://www.nature.com/reprints>

Publisher's note Springer Nature remains neutral with regard to jurisdictional claims in published maps and institutional affiliations.



Open Access This article is licensed under a Creative Commons Attribution 4.0 International License, which permits use, sharing, adaptation, distribution and reproduction in any medium or format, as long as you give

appropriate credit to the original author(s) and the source, provide a link to the Creative Commons license, and indicate if changes were made. The images or other third party material in this article are included in the article's Creative Commons license, unless indicated otherwise in a credit line to the material. If material is not included in the article's Creative Commons license and your intended use is not permitted by statutory regulation or exceeds the permitted use, you will need to obtain permission directly from the copyright holder. To view a copy of this license, visit <http://creativecommons.org/licenses/by/4.0/>.

© The Author(s) 2022